ECS Electrochemistry Letters, **3** (4) D1-D2 (2014)
2162-8726/2014/3(4)/D1/2/$31.00 © The Electrochemical Society

Effects of Fluorinated Surfactant in Cathodic Deposition of TiO_2 Films with Supercritical CO_2 Emulsified Electrolyte

Tso-Fu Mark Chang,[a,*,z] Wei-Hao Lin,[a,b] Yung-Jung Hsu,[b] Tatsuo Sato,[a] and Masato Sone[a]

[a]*Precision and Intelligence Laboratory, Tokyo Institute of Technology, Midori-ku, Yokohama 226-8503 Japan*
[b]*Department of Materials Science and Engineering, National Chiao Tung University, Hsinchu, Taiwan 30010, China*

Effect of a fluorinated surfactant, $F(CF(CF_3)CF_2O)_3CF(CF_3)COO(CH_2CH_2O)CH_3$, in pore structure and grain size of the TiO_2 films deposited cathodically was studied. Increase in pore size and decrease in grain size were observed when the fluorinated surfactant was used. When supercritical CO_2 was introduced into the system, synergetic effect on increasing the pore size was observed. Also, grain coarsening was observed for the films deposited with supercritical CO_2. Therefore, the fluorinated surfactant combining with supercritical CO_2 demonstrated the ability to control morphology and grain size of the deposited TiO_2 films at the same time.
© 2014 The Electrochemical Society. [DOI: 10.1149/2.003404eel] All rights reserved.

Manuscript submitted December 5, 2013; revised manuscript received January 17, 2014. Published January 25, 2014.

Applications of TiO_2 in various fields of technology, such as solar cell, photocatalysis, hydrogen generation, and gas sensing are highly dependent on morphology of the TiO_2 fabricated.[1] TiO_2 films can be fabricated by chemical vapor deposition,[2] sol-gel method,[3] spray pyrolysis,[4] and hydrothermal reaction.[5] Among the different synthetic routes, cathodic deposition offers a low-cost yet effective process for fabrication of TiO_2 films. TiO_2 films cathodically deposited have been reported be porous.[6–8] Formation of the pores is suggested to be caused by gases formed during the deposition process.[7] Possible gas evolution reactions are shown in the following.

$$2H_2O + 2e^- \rightarrow 2OH^- + H_2 \quad [1]$$

$$2NO_3^- + 6H_2O + 10e^- \rightarrow 12OH^- + N_2 \quad [2]$$

$$NO_3^- + 6H_2O + 8e^- \rightarrow 9OH^- + NH_3 \quad [3]$$

Emulsifying the aqueous electrolyte with supercritical CO_2 (sc-CO_2) and a surfactant has been reported to be effective in controlling properties of the TiO_2 films deposited,[9] and properties of the films deposited are suggested to be highly dependent on the properties, especially size, of the dispersed phase in the sc-CO_2 emulsion.[9–11] Lee et al. reported nano-scale dispersed phase can be formed when a fluorinated surfactant (F-surf) is used.[12] Rahman et al. reported morphology of Ni films electrodeposited can be varied from smooth to porous simply by using a F-surf similar to the one used in Lee et al.'s study.[12,13] The same F-surf will be used in this study to examine the effects on morphology and grain size of the TiO_2 films deposited with sc-CO_2 emulsified $TiCl_3$+$NaNO_3$ electrolyte.

Experimental

The base electrolyte was composed of 0.47 M NaCl, 25 mM $TiCl_3$, and 75 mM $NaNO_3$. The F-surf used was $F(CF(CF_3)CF_2O)_3CF(CF_3)COO(CH_2CH_2O)CH_3$. The deposition with only the base electrolyte is denoted as conventional deposition (CONV-0 μL). Deposition with addition of 20 μL of the F-surf is denoted as CONV-20 μL. Three volumes of the F-surf were used for the deposition with sc-CO_2 (10 MPa and 20 vol.%), which were 0 (DSCE-0 μL), 20 μL (DSCE-20 μL), and 40 μL (DSCE-40 μL). Temperature used for all deposition processes was 40°C. Current density of 25 mA/cm^2 and deposition time of 10 min were used for all the deposition processes. The samples were heat-treated in air at 400°C for 1 hr before further analysis. Morphology of the films was examined by a scanning electron microscope (SEM). Crystal structural analysis was conducted by X-ray diffraction (XRD) at a glancing angle of 2.0°. Grain size was calculated using Scherrer equation.

Results and Discussion

Morphology of TiO_2 film fabricated by CONV-0 μL was porous and composed of nano-sacle particles and micro-scale aggregates, shown in Fig. 1a. Size of most of the pores was in nano-scale, and some pores had size in several hundreds of nanometer. Number of pores having size in several hundreds of nanometer increased after addition of the F-surf as shown in Fig. 1b. Evolution rate of the gases causing formation of the pores should be about the same between CONV-0 μL and CONV-20 μL since the gas evolution reactions are mostly related to temperature,[7] and the temperature was fixed at 40°C. Therefore, the increase in size of the pores should be related to the F-surf. Addition of the F-surf could form micelles solubilizing gases produced from reaction 1–3, and the micelles could adsorb on surface of cathode to form large pores.[14]

Size of the pores and the aggregates both increased when sc-CO_2 (DSCE-0 μL) was used, shown in Fig. 1c. The large pores were suggested to be caused by demoted desorption rate of the gas bubbles from the surface cathode, which is a result of lowered buoyancy force caused by the high pressure. Size of the pores further increased after addition of the F-surf (DSCE-20 μL), as shown in Fig. 1d. Size of the dispersed phase solubilizing sc-CO_2 is expected to be in nano-scale.[12] Size of the pores formed in DSCE-20 μL was much larger than the expected size of the dispersed phase. This indicated the pores were not formed by adsorption of the dispersed phase on the surface of cathode. Similar results were reported in the study on Ni electroplating with the same F-surf, where pore size much larger than the expected disperse phase size was observed.[13] Therefore, we suggest the large pores observed were formed by adsorption of micelles mainly composed of gases (H_2, N_2, and NH_3) produced from reaction 1–3. The mechanism is similar to fabrication of porous films with a gas-template.[14] In addition, size of the pores in DSCE-20 μL was larger than the case in CONV-20 μL, which indicates adsorption strength of the micelles were stronger because of the lowered buoyancy force. Morphology of the TiO_2 film did not vary much when 40 μL of the F-surf was used, shown in Fig. 1e.

The TiO_2 films were confirmed to be anatase structure from XRD analysis. XRD peak corresponded to the (101) facet was used in calculation of the grain size. Grain refinement was observed after addition of the F-surf as shown in Fig. 2. Chemical reactions involved in cathodic deposition of TiO_2 are shown in the following.

$$Ti^{3+} + NO_3^- \rightarrow TiO^{2+} + NO_2 \quad [4]$$

$$TiO^{2+} + 2OH^- + xH_2O \rightarrow TiO(OH)_2 \cdot xH_2O \quad [5]$$

$$TiO(OH)_2 \rightarrow TiO_2 + H_2O \quad [6]$$

*Electrochemical Society Active Member.
zE-mail: chang.m.aa@m.titech.ac.jp

Downloaded on 2014-04-28 to IP 140.113.38.11 address. Redistribution subject to ECS terms of use (see ecsdl.org/site/terms_use) unless CC License in place (see abstract).

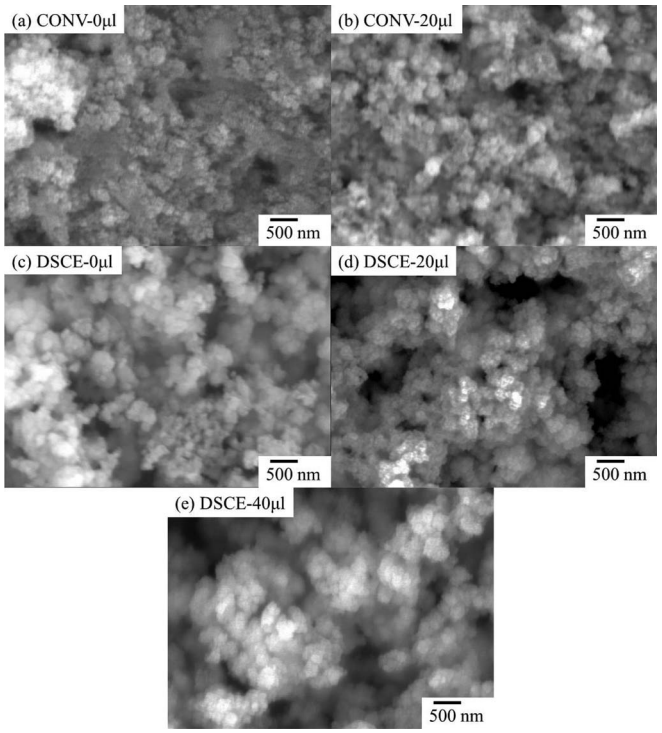

Figure 1. SEM micrographs of the TiO_2 films fabricated by (a) conventional deposition without addition of any surfactant (CONV-0 μL), (b) conventional deposition with 20 μL of the surfactant (CONV-20 μL), (c) deposition with sc-CO_2 at 10 MPa (DSCE-0 μL), (d) deposition with sc-CO_2 emulsified electrolyte and 20 μL of the surfactant (DSCE-20 μL), and (e) deposition with sc-CO_2 emulsified electrolyte and 40 μL of the surfactant (DSCE-40 μL).

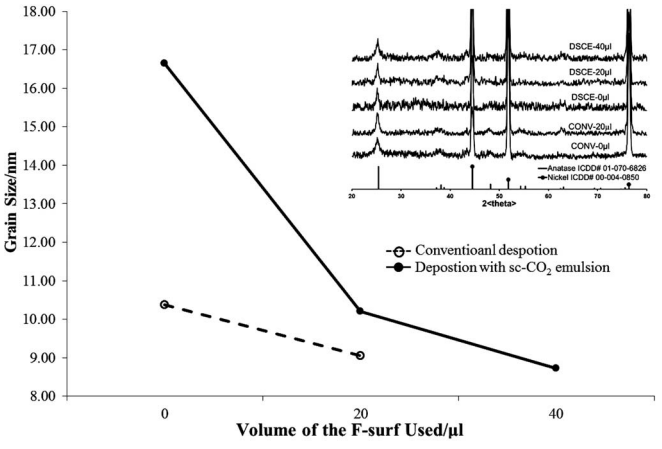

Figure 2. Grain size of the TiO_2 films deposited under different conditions. The embedded image shows XRD patterns of TiO_2 deposited under different conditions.

Size of the TiO_2 grains obtained is highly related to electrogeneration rate of the hydroxyl ions in reaction 1–3 and size of the oxy-hydroxyl-Ti particles produced in reaction 5.[7,15] High hydroxyl ions electrogeneration rate would lead to formation of large oxy-hydroxyl-Ti particles, which then cause formation of large TiO_2 grains. The F-surf could adsorb on the surface of cathode to cause an inhibiting effect on electrogeneration of the hydroxyl ions. Therefore, the inhibiting effect caused the grain refinement effect.

Grain coarsening was observed when sc-CO_2 was used, where grain size increased from 10.38 nm (CONV-0 μL) to 16.65 nm (DSCE-0 μL), shown in Fig. 2. Increase in pressure can cause a decrease in self-diffusivity and increase in viscosity of the aqueous electrolyte. These would lower transfer efficiency of TiO^{2+} to the surface of cathode and cause a reduction in nucleation density of the oxy-hydroxyl-Ti particles and an increase in size of the oxy-hydroxyl-Ti particles formed, which then lead to the grain coarsening effect. The sc-CO_2 emulsion is expected to give periodic-plating-characteristic as reported in previous study,[9–11] which would promote electrogeneration of hydroxyl ions and lead to the grain coarsening effect.[9] However, size of the dispersed phase formed with the F-surf was too small to give the effect of periodic-plating-characteristic.[16] Instead, addition of the F-surf led to inhibiting effect of the electrochemical reactions involved and the grain refinement effect.

Conclusions

Increase in pore size of the TiO_2 films deposited was observed when the F-surf and sc-CO_2 were used. Grain size of the TiO_2 was decreased after addition of the F-surf. On the other hand, grain coarsening effect was observed when sc-CO_2 was used. Therefore, the results showed that both pore structure and grain size of the TiO_2 films could be controlled simultaneously or separately by utilizing the F-surf and sc-CO_2.

Acknowledgment

Funding Program for Next Generation World-leading Researchers (NEXT Program) GN037, Cabinet Office (CAO), Japan.

References

1. X. Chen and S. S. Mao, *Chem. Rev.*, **107**, 2891 (2007).
2. W. J. Lee and Y. M. Sung, *Cryst. Growth Des.*, **12**, 5792 (2012).
3. S. Lee, I. S. Cho, J. H. Lee, D. H. Kim, D. W. Kim, J. Y. Kim, H. Shin, J. K. Lee, H. S. Jung, N. G. Park, K. Kim, M. J. Ko, and K. S. Hong, *Chem. Mater.*, **22**,1958 (2010).
4. E. L. Unger, E. Ripaud, P. Leriche, A. Cravino, J. Roncali, E. M. J. Johansson, A. Hagfeldt, and G. Boschloo, *J. Phys. Chem. C*, **114**, 11659 (2010).
5. A. Nakahira, T. Kubo, and C. Numako, *Inorg. Chem.*, **49**, 5845 (2010).
6. C. C. Hu, C. C. Huang, and K. H. Chang, *Electrochem. Commun.*, **11**, 434 (2009).
7. C. C. Huang, H. C. Hsu, C. C. Hu, K. H. Chang, and Y. F. Lee, *Electrochim. Acta*, **55**, 7028 (2010).
8. C. C. Hu, H. C. Hsu, and K. H. Chang, *J. Electrochem. Soc.*, **159**, D418 (2012).
9. T. F. M. Chang, W. H. Lin, Y. J. Hsu, C. Y. Chen, T. Sato, and M. Sone, *Electrochem. Commun.*, **33**, 68 (2013).
10. T. F. M. Chang, M. Sone, A. Shibata, C. Ishiyama, and Y. Higo, *Electrochim. Acta*, **55**, 6469 (2010).
11. T. F. M. Chang and M. Sone, *Surf. Coat. Technol.*, **205**, 3890 (2011).
12. C. T. Lee Jr., W. Ryoo, P. G. Smith Jr., J. Arellano, D. R. Mitchell, R. J. Lagow, S. E. Webber, and K. P. Johnston, *J. Am. Chem. Soc.*, **125**, 3181 (2003).
13. Md. M. Rahman, M. Sone, H. Uchiyama, M. Sakurai, S. Miyata, T. Nagai, Y. Higo, and H. Kameyama, *Surf. Coat. Technol.*, **201**, 7513 (2007).
14. Y. Li, W. Z. Jia, Y. Y. Song, and X. H. Xia, *Chem. Mater.*, **19**, 5758 (2007).
15. I. N. Kholmanov, E. Barborini, S. Vinati, P. Piseri, A. Podestà, C. Ducati, C. Lenardi, and P. Milani, *Nanotechnology*, **14**, 1168 (2003).
16. T. F. M. Chang, T. Shimizu, C. Ishiyama, and M. Sone, *Thin Solid Films*, **529**, 25 (2013).

Downloaded on 2014-04-28 to IP 140.113.38.11 address. Redistribution subject to ECS terms of use (see ecsdl.org/site/terms_use) unless CC License in place (see abstract).